International Journal of Thermal Sciences 49 (2010) 714–720

Contents lists available at ScienceDirect

International Journal of Thermal Sciences

journal homepage: www.elsevier.com/locate/ijts

Carrier-extraction from two rigid spheres in tandem

Gheorghe Juncu*

POLITEHNICA University Bucharest, Catedra Inginerie Chimica, Polizu 1, 78126 Bucharest, Romania

ARTICLE INFO

Article history:
Received 30 March 2009
Received in revised form
4 September 2009
Accepted 28 September 2009
Available online 14 October 2009

Keywords:
Mass transfer
Carrier-extraction
Two spheres in tandem
Reversible chemical reaction
Creeping flow

ABSTRACT

Unsteady mass transfer between two rigid spheres in tandem and a surrounding fluid flow with reversible second-order chemical reaction on the surface of the spheres has been analysed. The spheres have the same diameter and initial concentration. The dispersed phase reactant and product are insoluble in the continuous phase. The continuous phase reactant and product are insoluble in the dispersed phase. Axisymmetric, slow, viscous flow (Stokes flow) around the spheres was considered. The mass balance equations were solved numerically in spherical/bispherical coordinates systems by a finite difference nonlinear multigrid method. For moderate Pe number, $Pe = 100$, modified Hatta modulus, $Ha^2 = 10, 100, 1000$, and different values of the diffusion coefficients, the computations focused on the influence of the spheres spacing on the mass transfer rates.

1. Introduction

Carrier-extraction [1] is a versatile technology with a wide range of commercial applications. It is utilized in the processing of metals and nuclear fuels (hydrometallurgy), pharmaceuticals and agricultural chemicals. It is also an important operation in industrial wastewater treatment, food processing and the recovery of biomolecules from fermentation broth. An overview of the carrier-extraction applications in industry, life and environmental sciences can be viewed in [1–5].

Carrier-extraction uses ion exchangers for separating the desired components. Because most ion exchangers are practically insoluble in the aqueous phase, the chemical reaction between the ion exchanger and the extracted component is assumed to take place on the interface. In almost all cases of practical interest, the chemical reaction is second-order, reversible.

Mass transfer from/to a single drop with chemical reaction on the surface of the drop was analysed theoretically (to our knowledge) only in [6,7] (a model based on film theory can be viewed in [8]). In real life applications, carrier-extraction is performed in liquid–liquid dispersions. The single sphere data cannot predict accurately the mass transfer rate in liquid–liquid dispersions for all situations. In this case, a first interest problem is the interaction between spheres which are moving in close proximity. A first step in the investigation of this interaction is the analysis of carrier-extraction from two spheres placed in a uniform viscous flow parallel to their line of centers (in tandem).

The analysis of carrier-extraction from two rigid spheres in tandem is the subject of this work. To our knowledge, this problem was not investigated until now. The forced convection heat/mass transfer around two/three spheres in tandem was analysed theoretically in [9–15]/[16–18]. In these studies the chemical reaction is not present. The hydrodynamic regime considered in this work is creeping flow. Moderate values of the Pe numbers, $Pe = 100$, were assumed. Three values of Ha^2 were considered, $Ha^2 = 10, 100, 1000$. The main problems investigated are: (1) the influence of the distance between the spheres on the mass transfer rates; (2) the influence of the interaction on the chemical composition on the surface of the spheres; (3) the influence of the diffusivity ratio on the mass transfer rates.

2. Basis equations and method of solution

Consider the steady, axisymmetric, creeping flow of a Newtonian incompressible fluid past two rigid spheres of equal diameter d, parallel to their line of centers. Oscillations and rotation of the spheres do not occur during the movement. The spheres have the same initial concentration. On the surface of the spheres, the second order, reversible chemical reaction

$$A + B \leftrightarrow C + E, \quad r = k[m_A m_B - (1/K_e) m_C m_E]$$

takes place. The reactant A and the product E are soluble only within the surrounding fluid (continuous phase). The reactant B

---

* Tel./fax: +40 21 345 0596.
E-mail addresses: juncu@easynet.ro, juncugh@netscape.net

1290-0729/$ – see front matter © 2009 Elsevier Masson SAS. All rights reserved.
doi:10.1016/j.ijthermalsci.2009.09.010

Nomenclature

A	dimensionless concentration of reactant present only in the surrounding fluid (continuous phase), $m_A/m_{A\infty}$
B	dimensionless concentration of reactant soluble only inside the spheres (dispersed phase), m_B/m_{B0}
c	characteristic length, bispherical coordinate system (m)
$\bar{c}$	dimensionless characteristic length, bispherical coordinate system, $2c/d$
C	dimensionless concentration of product soluble only inside the spheres (dispersed phase), m_C/m_{B0}
d	sphere diameter (m)
D_i	Fickean self-diffusion coefficient of the species i, $i = A$, B, C, E ($\mathrm{m^2\ s^{-1}}$)
D_{ref}	reference self-diffusion coefficient ($\mathrm{m^2\ s^{-1}}$)
E	dimensionless concentration of product soluble only in the surrounding fluid (continuous phase) $m_E/m_{A\infty}$
Ha	modified Hatta modulus, $Ha^2 = kd^2m_{B0}/4D_{\mathrm{ref}}$, dimensionless
k	forward chemical reaction rate constant ($\mathrm{m^3\ kg^{-1}\ s^{-1}}$) (transformed for bulk concentrations)
K_{e}	chemical equilibrium constant, dimensionless
L	distance from the center of the sphere to the origin of the bispherical coordinate system (m)
m_i	mass concentration of species i, $i = A$, B, C, E ($\mathrm{kg\ m^{-3}}$) (bulk values)
Pe	Peclet number, $Pe = U_\infty d/D_{\mathrm{ref}}$, dimensionless
q	dimensionless group, $q = m_{A\infty}/m_{B0}$
r	reaction rate ($\mathrm{kg\ m^{-3}\ s^{-1}}$) (transformed for bulk concentrations)
r^*	dimensionless radial coordinate, $2R/d$, in spherical coordinate system
R	radial coordinate, spherical coordinate system (m)
R_i	diffusivity ratio, D_i/D_{ref}, $i = A$, B, C, E, dimensionless
Re	Reynolds number based on the spheres diameter, $Re = U_\infty d/\nu$, dimensionless
Sc	Schmidt number, $Sc = \nu/D_{\mathrm{ref}}$, dimensionless
t	time (s)
U_∞	free stream velocity ($\mathrm{m\ s^{-1}}$)

Greek letters

δ	dimensionless distance from the center of the sphere to the origin of the bispherical coordinate system, $\delta = 2\ L/d$
η	coordinate in bispherical coordinate system
ξ	coordinate in bispherical coordinate system (rad)
ν	kinematic viscosity ($\mathrm{m^2\ s^{-1}}$)
θ	polar angle in spherical coordinate system (rad)
τ	dimensionless time or Fourier number, $\tau = 4tD_{\mathrm{ref}}/d^2$
ψ	dimensionless stream function

Subscripts

A	refers to reactant A
B	refers to reactant B
C	refers to product C
E	refers to product E
s	refers to the surface of the spheres
0	initial conditions
1	upstream (leading) sphere
2	downstream (trailing) sphere
∞	large distance from the spheres

and the product C are soluble only within the spheres (dispersed phase). Due to the complexity of the problem, the following supplementary assumptions are considered:

(i) during the mass transfer, the volume and the shape of the spheres remain constant (this implicitly means that the diameter of the spheres remains constant);
(ii) the physical properties are constant;
(iii) no phase change occurs;
(iv) the system is isothermal;
(v) the only diffusion mechanism is the Fick diffusion mechanism; cross-diffusion effects are neglected;
(vi) the effects of free and Marangoni convections are negligible.

The ion exchangers used frequently in carrier-extraction are tensioactive substances. From this reason, the assumption of spheres with rigid surfaces can be considered quite acceptable.

For mass transfer inside the spheres we used the axisymmetric spherical coordinate system (R, θ). For mass transfer in the surrounding fluid, it is convenient to use the bispherical coordinate system (ξ, η), [19–21]. The axisymmetric bispherical coordinate system (ξ, η) maps the physical domain occupied by the surrounding fluid into the rectangle $\eta_1 \le \eta \le \eta_2$, $0 \le \xi \le \pi$ ($\eta_1 < 0$, $\eta_2 > 0$). The surfaces of the spheres are located at $\eta = \eta_1$ and $\eta = \eta_2$. The relations between η_1, η_2, the diameters of the spheres, d_1, d_2, and the distances, L_1, L_2, of their centers from the origin of the coordinates system are:

$$\frac{d_i}{2} = \frac{c}{\sinh|\eta_i|};\ L_i = c\coth|\eta_i|, \quad i = 1,2$$

where $c > 0$ is a characteristic length. Obviously, if $d_1 = d_2 = d$, it results $\eta_1 = -\eta_2$ and $L_1 = L_2 = L$.

Under these assumptions, the dimensionless mathematical model equations (the radius of the spheres is considered the length scale, the free stream velocity U_∞ the velocity scale and the *diffusion time* $d^2/(4D_{\mathrm{ref}})$ the time scale), expressed in dimensionless spherical coordinate system (r^*, θ) (for the mass transfer inside the spheres) and in bispherical coordinate system (for mass transfer in the surrounding fluid), are:

- inside the spheres

$$\frac{\partial Z_i}{\partial \tau} = R_Z \Delta Z_i, \quad i = 1,2, \ Z = B,C \tag{1}$$

- in the surrounding fluid ($Z = A$, E)

$$\frac{\partial Z}{\partial \tau} + \frac{Pe}{2}\frac{G^3}{\sin\xi}\left(\frac{\partial \psi}{\partial \eta}\frac{\partial Z}{\partial \xi} - \frac{\partial \psi}{\partial \xi}\frac{\partial Z}{\partial \eta}\right) = R_Z\left[G^2\left(\frac{\partial^2 Z}{\partial \eta^2} + \frac{\partial^2 Z}{\partial \xi^2}\right) - \frac{G\sinh\eta}{\bar{c}}\frac{\partial Z}{\partial \eta} + \frac{G(\cosh\eta\cos\xi - 1)}{\bar{c}\sin\xi}\frac{\partial Z}{\partial \xi}\right] \tag{2}$$

where

$$\Delta = \frac{1}{r^{*2}}\frac{\partial}{\partial r^*}\left(r^{*2}\frac{\partial}{\partial r^*}\right) + \frac{1}{r^{*2}\sin\theta}\frac{\partial}{\partial \theta}\left(\sin\theta\frac{\partial}{\partial \theta}\right), \quad G = \frac{\cosh\eta - \cos\xi}{\bar{c}}$$

and ψ is the dimensionless stream function.

A reference diffusion coefficient, D_{ref}, was used to define the dimensionless time, τ, and the Peclet number, Pe. The reference diffusion coefficient can be the diffusion coefficients of any of the species A, B, C and E.

The boundary conditions to be satisfied are:

- spheres center ($r^* = 0$)

$$B_i, C_i = \text{finite}, \quad i = 1,2 \tag{3a}$$

- free stream ($\eta = \xi = 0$)

$$A = 1, \quad E = 0 \tag{3b}$$

- symmetry axis ($\theta = 0, \pi$) and ($\xi = 0$ and $\eta \neq 0, \xi = \pi$)

$$\frac{\partial A}{\partial \xi} = \frac{\partial E}{\partial \xi} = \frac{\partial B_i}{\partial \theta} = \frac{\partial C_i}{\partial \theta} = 0, \quad i = 1,2 \tag{3c}$$

- interface ($r^* = 1$) ($\eta = \eta_1$, $\eta = \eta_2$)

$$R_A \frac{\cosh\eta_i - \cos\xi}{\bar{c}} \left.\frac{\partial A}{\partial \eta}\right|_{\eta=\eta_i} = Ha^2\left(AB_i - \frac{1}{K_e} C_i E\right), \quad i = 1,2 \tag{4a}$$

$$R_B \frac{\partial B_i}{\partial r^*} = -Ha^2 q\left(AB_i - \frac{1}{K_e} C_i E\right), \quad i = 1,2 \tag{4b}$$

$$R_C \frac{\partial C_i}{\partial r^*} = Ha^2 q\left(AB_i - \frac{1}{K_e} C_i E\right), \quad i = 1,2 \tag{4c}$$

$$R_E \frac{\cosh\eta_i - \cos\xi}{\bar{c}} \left.\frac{\partial E}{\partial \eta}\right|_{\eta=\eta_i} = -Ha^2\left(AB_i - \frac{1}{K_e} C_i E\right), \quad i = 1,2 \tag{4d}$$

The dimensionless initial conditions are:

$$\tau = 0, \quad E = 0, \quad A = 1, \quad B_i = 1, \quad C_i = 0, \ i = 1,2 \tag{5a}$$

The quantities of interest used to characterize the unsteady mass transfer are: (1) spheres and surface of the spheres dimensionless concentrations and (2) local and overall instantaneous Sherwood numbers.

The dimensionless spheres average concentrations of the species B and C are computed with the relations:

$$\overline{Z}_i = \frac{3}{2}\int_0^{\pi}\int_0^{1} Z_i r^{*2} \sin\theta dr^* d\theta, \quad Z = B, C, \ i = 1,2 \tag{5b}$$

The dimensionless average surface concentrations are computed with the relations:

$$\overline{Z}_{i,s} = \frac{1}{2}\int_0^{\pi} Z_i|_{r^*=1} \sin\theta d\theta, \quad Z = B, C, \ i = 1,2 \tag{6a}$$

and

$$\overline{Z}_{i,s} = \frac{\sinh\eta_i}{2}\int_0^{\pi} Z_i|_{\eta=\eta_i} \frac{\sin\xi}{\cosh\eta_i - \cos\xi} d\xi, \quad Z = A, E, \ i = 1,2 \tag{6b}$$

Considering the diameter of the sphere as characteristic length and the instantaneous dimensionless concentration difference, $(\overline{Z}_i - \overline{Z}_{i,s})$, $Z = B$, C, $i = 1$, 2, as driving force, $Sh_{Z,i}(\theta)$ and $Sh_{Z,i}$, were calculated by the relations:

$$Sh_{Z,i}(\theta) = -\frac{2}{\overline{Z}_i - \overline{Z}_{i,s}} \left.\frac{\partial Z_i}{\partial r^*}\right|_{r^*=1}, \quad Z = B, C, \ i = 1,2 \tag{7a}$$

$$Sh_{Z,i} = \frac{1}{2}\int_0^{\pi} Sh_{Z,i}(\theta) \sin\theta d\theta, \quad Z = B, C, \ i = 1,2 \tag{7b}$$

Considering the diameter of the sphere as characteristic length and the instantaneous dimensionless concentration difference, $(Z_\infty - \overline{Z}_{i,s})$, $Z = A$, E, $i = 1$, 2 as driving force, $Sh_{Z,i}(\xi)$ and $Sh_{Z,i}$, were calculated by the relations:

$$Sh_{Z,i}(\xi) = \pm \frac{2}{Z_\infty - \overline{Z}_{i,s}} \left.\frac{\partial Z_i}{\partial \eta}\right|_{\eta=\eta_i} \frac{\cosh\eta_i - \cos\xi}{\bar{c}}, \quad Z = A, E, \ i = 1,2 \tag{8a}$$

$$Sh_{Z,i} = \pm \frac{1}{Z_\infty - \overline{Z}_{i,s}} \frac{\sinh\eta_i}{\bar{c}} \int_0^{\pi} \left.\frac{\partial Z}{\partial \eta}\right|_{\eta=\eta_i} \frac{\sin\xi}{\cosh\eta_i - \cos\xi} d\xi, \quad Z = A, E, \ i = 1,2 \tag{8b}$$

The values of the dimensionless stream function were calculated numerically in [22]. The mass balance equations were solved numerically. Inside the spheres the central finite difference scheme was used to discretize the spatial derivatives. The spatial derivatives of equation (2) were approximated by the exponentially fitted finite difference scheme [23]. Numerical experiments were made with the spatial discretization steps, $\Delta r^* = \Delta\eta = 1/128, 1/256, 1/512$ and $\Delta\theta = \Delta\xi = \pi/128$, $\pi/256$ and $\pi/512$. For the time discretization the backward, second order accurate scheme, coupled with a fully implicit treatment of the spatial derivatives was used.

The numerical method used to solve the discrete parabolic equations is the parabolic nonlinear multigrid (MG) algorithm [24] already presented in [7]. We considered that it is not necessary to repeat its description here. It must be mentioned that, for the parameters values used in this work, the results obtained on a mesh with 129 × 129 points in each phase can be considered mesh independent.

3. Results

The dimensionless equations (1) and (2) and the boundary and initial conditions (3)–(5) depend on eight dimensionless parameters: Ha^2, K_e, $\delta = 2L/d$, Pe, q and three diffusivity ratios.

The value considered for Pe is $Pe = 100$. For usual liquids, the Schmidt number, Sc, is around $10^2 - 10^3$. For $Sc \sim O(10^2 - 10^3)$ and creeping flow (i.e. $Re < 1$), the product $ReSc = Pe$ is $Pe < 1000$. The values considered for the modified Hatta modulus, Ha^2, are $Ha^2 = 10$, 100 and 1000. The arguments for this selection were discussed in [7]. The parameter q takes the values 1, 5 and 10. The chemical equilibrium constant K_e was considered equal to 1, 10, 100 and ∞ (irreversible chemical reaction). The values considered for the diffusivity ratios R_Z are in the range 0.5–2.0 (inside and outside the spheres the diffusion mechanism obeys Stokes–Einstein or Eyring theories).

Before presenting and discussing the results obtained in this work, it should be mentioned that: (a) for Stokes flow around two equal-sized spheres in tandem, the stream function is symmetric about an axis perpendicular in $\eta = 0$ to the spheres centreline;

(b) the spheres have identical values for the drag coefficients, surface pressure, vorticity and so on; (*c*) the present results are not affected by the hydrodynamic tandem interaction phenomena that occur in Navier–Stokes flow.

The main aim of any work dedicated to heat/mass transfer around two (at least) bodies submerged into a flowing fluid is to find the rules of interaction. In all the previous articles dedicated to the heat/mass transfer from two spheres in tandem, [9–15], the surrounding fluid controls the transfer. The tandem interaction is described by the following rules (valid especially for spheres with constant concentration/temperature):

- the values of the *Sh* number for both spheres are smaller than the value of the *Sh* number for the isolated sphere; the interaction effects are stronger for the downstream sphere;
- the increase in spheres spacing decreases the interaction effects.

The target of the present process is the extraction of species *B* from the spheres. Chemical species that are soluble only in the ambient fluid are involved in this process. Thus, one of the first questions that arise is: can we use the previously mentioned rules to describe the present process?

The first numerical simulations were made considering the diffusivity ratios equal to one, $R_Z = 1$, for $Z = A, B, C, E$, $q = 1$ and $K_e = 1$. For these parameters values, the influence of the spheres spacing on the mass transfer is presented in Figs. 1–3. We selected for graphical presentation only $\overline{B}_i, \overline{E}_{i,s}$, $Sh_{B,i}$ and $Sh_{E,i}$. It must be mentioned that, for the parameters values mentioned previously, $Sh_{C,i} \equiv Sh_{B,i}$, $\overline{C}_i = 1 - \overline{B}_i$, $\overline{C}_{i,s} = 1 - \overline{B}_{i,s}$, $Sh_{E,i} \equiv Sh_{A,i}$ and $\overline{E}_{i,s} = 1 - \overline{A}_{i,s}$. Figs. 1 and 2 show the results obtained for $Ha^2 = 100$. In Fig. 3 the data obtained for $Ha^2 = 10$ are presented. The results obtained for $Ha^2 = 1000$ are similar to those depicted in Figs. 1 and 2. For this reason we did not present these data. The discontinuity in the time variation of trailing sphere *Sh* numbers is due to the occurrence of negative values. Also, it must be mentioned that for $Ha^2 = 10$, negative values of the downstream sphere *Sh* numbers were observed for $\delta > 11$ ($\delta = 21$, for example).

Fig. 2 shows that it is very difficult to establish any connection between the present results for species *E* and the data presented in [9–15]. In reference [15] the connection between the time variations of the concentration of the transferring species and *Sh* numbers is very clear. For the present process, for example, Fig. 2b shows that the influence of δ on $Sh_{E,1}$ is negligible while Fig. 2a shows that the influence of δ on $\overline{E}_{1,s}$ is not negligible.

The present *Sh* number is not a direct measure of the intensity of the process. It is the ratio of two instantaneous average quantities: dimensionless concentration gradient on the surface of the sphere and dimensionless driving force (dimensionless concentration difference: average drop – average surface or average surface – free stream). It is widely used because it has a nonzero asymptotic limit; this asymptotic value is reached when the dimensionless driving force and the dimensionless concentration gradient on the surface of the sphere obey the same exponential decrease in time. In physical processes the surface concentration is usually considered constant or it is the result of a mass balance equation. In these cases it is not difficult to establish a direct connection between the asymptotic *Sh* value and the mass transfer rate. For the present process, the surface concentration is the resultant of the action of two phenomena: mass transfer (in both phases) and chemical reaction. The time variation of the surface concentration does not obey, in this case, simple, elementary rules. Situations like different asymptotic *Sh* values for approximately equal surface mass fluxes but different driving forces or approximately equal asymptotic *Sh* values for different surface mass fluxes and different driving forces, may occur. Under these conditions, for the present process, the mass transfer rates should be analysed in terms of the time variation of the average concentrations.

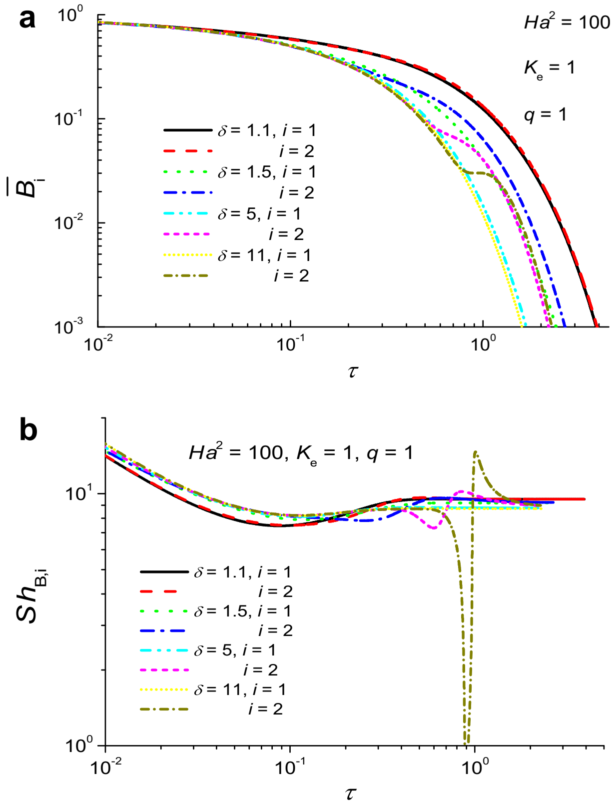

Fig. 1. Time evolution of the sphere average dimensionless concentration of species *B* and average *Sh* numbers for different spheres spacing and $Ha^2 = 100$; (a) $\overline{B}_i$; (b) $Sh_{B,i}$.

Concerning the influence of δ on the time variation of the dimensionless concentration of the chemical species *B*, Figs. 1 and 3 show that:

- the increase in δ increases the mass transfer rate inside the spheres;
- for very small values of δ, i.e. $\delta = 1.10$, the mass transfer rate inside the spheres is practically equal;
- for $\delta > 1.10$, the mass transfer inside the spheres is different; the mass transfer rate is higher inside the leading sphere;
- for $\delta \geq 5$, the influence of the spheres spacing on the mass transfer rate inside the spheres is not significant;
- the rules mentioned previously do not change for Ha^2 varying in the range 10–10^3.

The previous statements describe globally the interaction. The elementary steps (stages) of the process are:

- for very short times, in the diffusion regime, the interaction effects are not present; the mass transfer rates for both spheres are the same;
- the first interaction effects were observed for species *A*; when the chemical reaction starts, reactant *A* on the surface of the spheres is consumed; due to the geometry of the system and the flow direction, the surface of the trailing sphere is supplied with a larger amount of *A* than the surface of the leading sphere; the chemical reaction rate and implicitly the mass transfer rate on the surface of the trailing sphere are higher

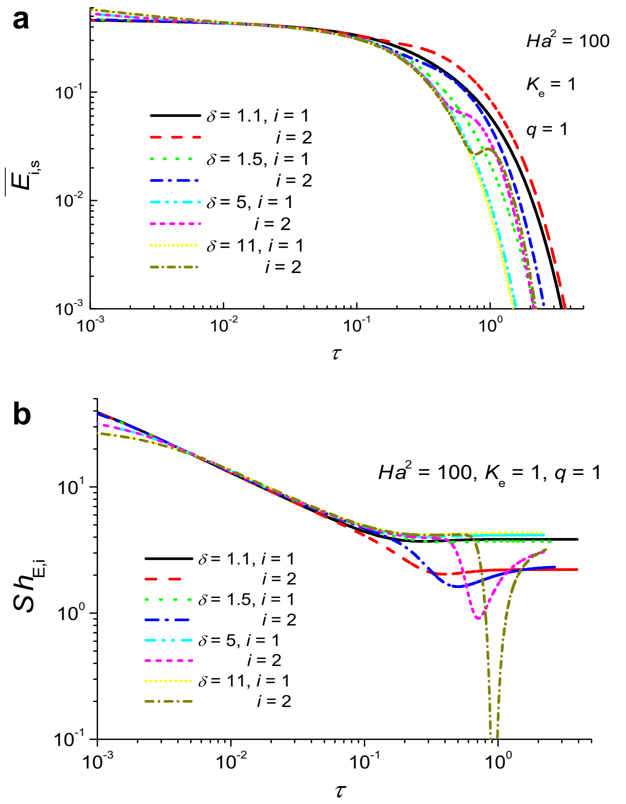

Fig. 2. Time evolution of the sphere surface average dimensionless concentration of species *E* and average *Sh* numbers for different spheres spacing and $Ha^2 = 100$; (a) $\overline{E}_{i,s}$; (b) $Sh_{E,i}$.

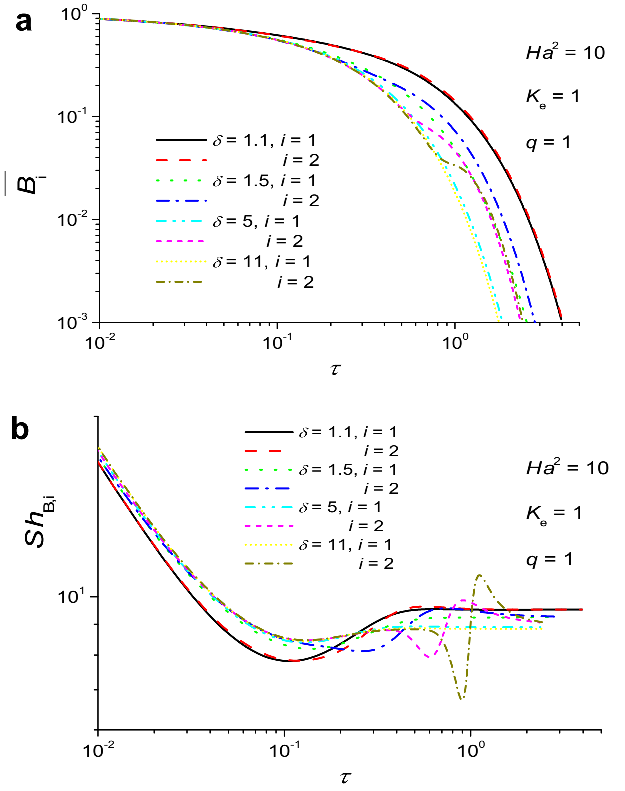

Fig. 3. Time evolution of the sphere average dimensionless concentration of species *B* and average *Sh* numbers for different spheres spacing and $Ha^2 = 10$; (a) $\overline{B}_i$; (b) $Sh_{B,i}$.

than on the surface of the leading sphere; this phenomenon does not take long times, it cannot be observed very well in Figs. 1–3 but it exists;

- the chemical species *E* generates the strongest interaction effects; the interaction effects depend on the surface and bulk *E* values (of course we refer to values during interaction); for very small values of spheres spacing the surface *E* values are greater than the bulk values; the spheres blocked each-other; the mass transfer rate decreases but is practically the same inside both spheres; the increase in δ decreases the values of $E_{2,s}$ when interaction starts; if the bulk values are comparable with the $E_{2,s}$ values, the chemical reaction rate on the surface of the downstream sphere drastically slows down and, in some situations, it reverses its sense; negative values of the *Sh* numbers occur in this case.

The next step of the present work is the analysis of the influence of the initial concentration ratio *q* and the chemical equilibrium constant, K_e, on the mass transfer rates. For the present process, the influence of *q* and K_e on the mass transfer rates follows the same rules as in [7]. The increase in *q* and K_e increases the mass transfer rates. Also, the variation in *q* and K_e does not change the interaction rules previously presented. For this reason we considered that a detailed presentation and discussion of these results in this work is not justified. From the numerical experiments made we selected for presentation the data plotted in Figs. 4 and 5. In Figs. 4 and 5 the curves symbolized by $Ha^2 = 0$ show the results obtained for mass

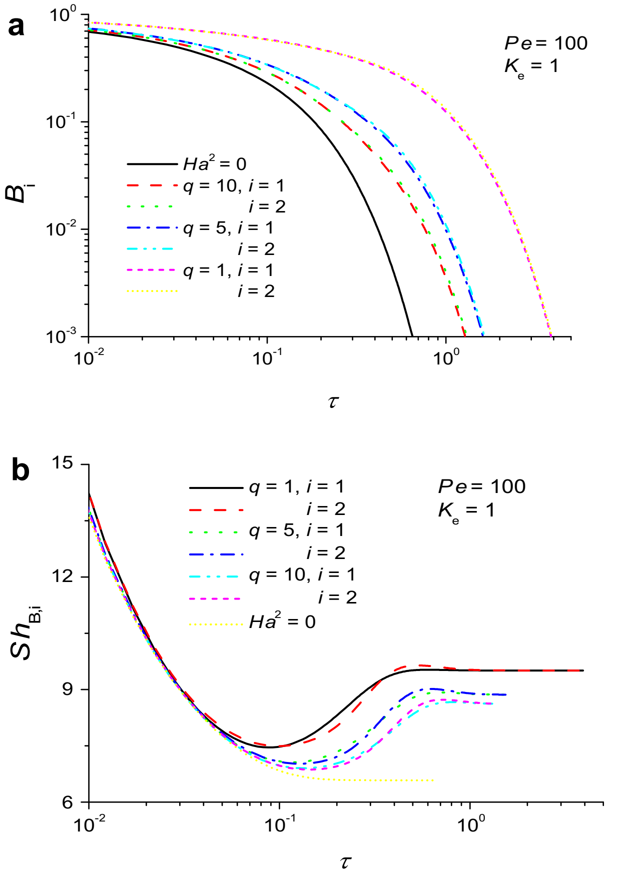

Fig. 4. The influence of the initial concentration ratio on the time evolution of the sphere average dimensionless concentration of species *B* and average *Sh* numbers for $\delta = 1.1$; (a) $\overline{B}_i$; (b) $Sh_{B,i}$.

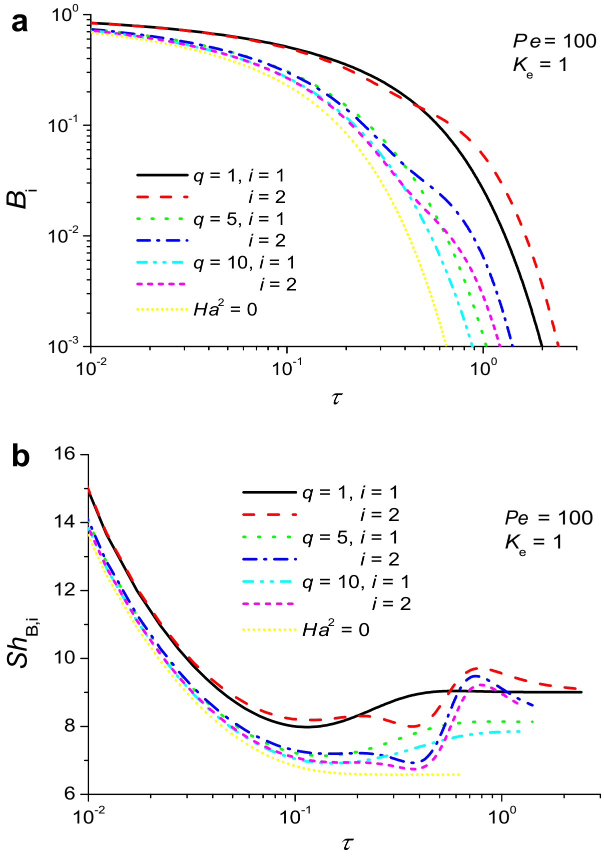

Fig. 5. The influence of the initial concentration ratio on the time evolution of the sphere average dimensionless concentration of species B and average Sh numbers for $\delta = 2$; (a) $\overline{B}_i$; (b) $Sh_{B,i}$.

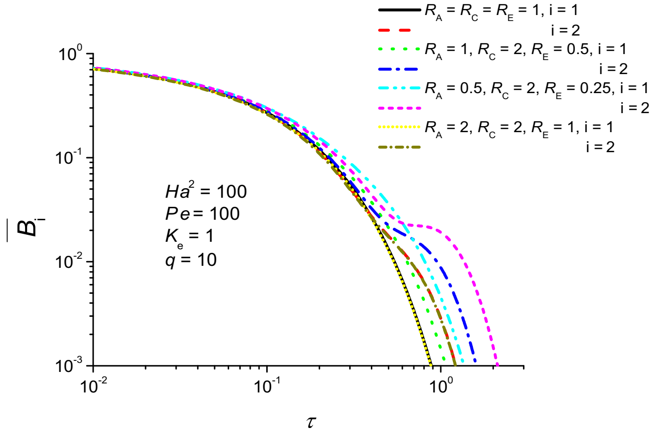

Fig. 7. The influence of the diffusivities ratios on the time evolution of the sphere average dimensionless concentration of species B for $\delta = 2$.

transfer without chemical reaction (i.e. the boundary conditions on the surface of the spheres are, $E_{i,s} = 1, A_{i,s} = 0, B_{i,s} = 0, C_{i,s} = 1, i = 1, 2$).

In Stokes–Einstein or Eyring theories, the diffusion coefficient of a solute into a solvent depends on its molar volume. In almost all cases of practical interest in carrier-extraction, the product C has a molar volume smaller than that of reactant B and the product E has a molar volume greater than that of reactant A. Based on these data, we considered $D_C = 2D_B$ and $D_E = 0.5D_A$. The diffusion coefficient of the reactant B was considered the *reference diffusion coefficient*. Thus, the only problem that remains is the selection of the values for R_A. From the possible combinations that can be made, we selected for presentation the following cases: (1) $D_A = D_B \Rightarrow R_A = 1$; (2) $D_A = 2D_B \Rightarrow R_A = 2$; (3) $D_A = 0.5D_B \Rightarrow R_A = 0.5$. To emphasize the effect of the diffusivities ratios on the mass transfer rates inside the spheres, the results obtained for $R_Z = 1$, $Z = A, B, C, E$, will be also presented.

The presence of the chemical species C and E on the interface is not desired because they decrease the rate of chemical reaction and implicitly the mass transfer rate. They are removed from the surface of the spheres by diffusion. The increase/decrease in the diffusion coefficients of the products increases/decreases the rate of chemical reaction and implicitly the mass transfer rates. Figs. 6–8 show that: (a) for $R_E = 1$, and $R_A = R_C = 1$, or $R_A = R_C = 2$, the mass transfer rates inside the spheres are practically equal; (b) the decrease in R_E decreases significantly the mass transfer rates inside the spheres even for $q = 10$. We may state that for the mass transfer rate inside the spheres the diffusivity of the product soluble only in the surrounding fluid is a key parameter. Also, we observed that the interaction rules derived previously for equal diffusivities remain valid.

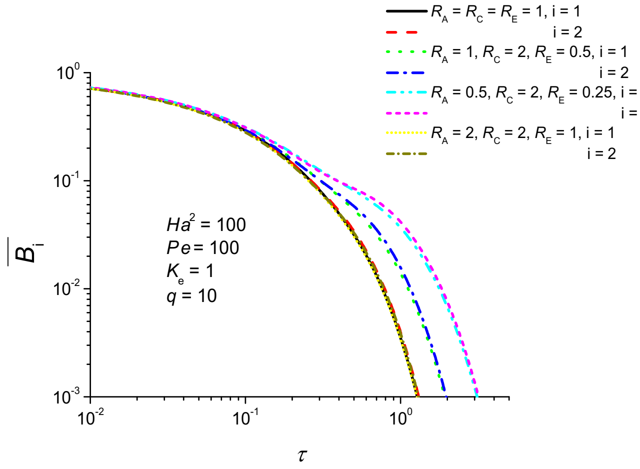

Fig. 6. The influence of the diffusivities ratios on the time evolution of the sphere average dimensionless concentration of species B for $\delta = 1.1$.

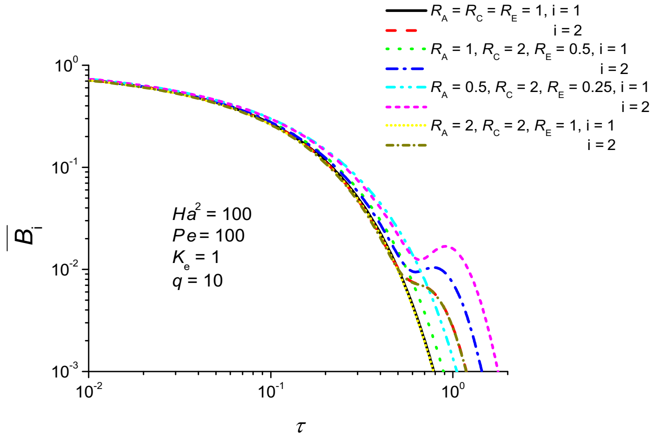

Fig. 8. The influence of the diffusivities ratios on the time evolution of the sphere average dimensionless concentration of species B for $\delta = 5$.

4. Conclusions

This work investigated numerically the carrier-extraction from two spheres in tandem. The spheres have the same diameter, initial composition and physical properties. Stokes flow around the spheres was assumed. The influence of spheres spacing on the mass transfer inside the spheres was investigated for moderate values of the *Pe* number and *Ha* modulus.

The present numerical results show that: (1) the increase in spheres spacing increases the mass transfer rate inside the spheres; (2) for very small values of spheres spacing the mass transfer rate inside the spheres is practically the same; (3) the increase in the spheres spacing increases the difference between the mass transfer rate inside the spheres; the mass transfer rate inside the upstream sphere is greater than inside the downstream sphere; (4) for $\delta \geq 5$, the influence of the spheres spacing on the mass transfer rate inside the spheres becomes less significant; (5) the increase in the initial concentration ratio and the chemical equilibrium constant increases the mass transfer rates inside the spheres; (6) the diffusion coefficient of the product soluble only in the surrounding fluid has a strong influence on the mass transfer rates inside the spheres.

References

[1] K. Schügerl, R. Hänsel, E. Schlichting, W. Halwachs, Reactive extraction. Int. Chem. Eng. 28 (1988) 393–405.
[2] L.K. Doraiswamy, M.M. Sharma, Heterogeneous Reactions: Analysis, Examples, Reactor Design, , In: Fluid–Fluid–Solid Reactions, vol. 2. Wiley, New York, 1984.
[3] M. Cox, Solvent extraction in hydrometallurgy. in: J. Rydberg (Ed.), Principles and Practice of Solvent Extraction. Marcel Dekker, New York, 1992, pp. 357–412.
[4] H.J. Bart, Reactive Extraction. Springer, Berlin, 2001.
[5] W. Halwachs, Reactive Extraction (2009).http://www.halwachs.de/reactive-extraction.htm.
[6] K. Inoue, F. Nakashio, Mass transfer accompanied by chemical reaction at the surface of a single droplet. Chem. Eng. Sci. 34 (1979) 191–197.
[7] Gh. Juncu, Unsteady mass transfer from/to a drop accompanied by a reversible second-order chemical reaction on the surface of the drop. Int. J. Thermal Sci. 47 (2008) 1294–1305.
[8] H. Klocker, H.J. Bart, R. Marr, H. Mueller, Mass transfer based on chemical potential theory: $ZnSO_4/H_2SO_4$/D2EHPA. AIChE. J. 43 (1997) 2479–2487.
[9] K. Aminzadeh, T.R. al Taha, A.R.H. Cornish, M.S. Kolansky, R. Pfeffer, Mass transport around two spheres at low Reynolds numbers. Int. J. Heat Mass Transfer 17 (1974) 1425–1436.
[10] R. Tal (Thau), D.N. Lee, W.A. Sirignano, Heat and momentum transfer around a pair of spheres in viscous flow. Int. J. Heat Mass Transfer 27 (1984) 1953–1962.
[11] C.K. Chen, K.L. Wong, S.C. Lee, The finite element solution of laminar combined convection from two spheres in tandem arrangement. Comput. Meth. Appl. Mech. Eng. 59 (1986) 73–84.
[12] C.H. Chiang, W.A. Sirignano, Interacting, convecting, vaporizing fuel droplets with variable properties. Int. J. Heat Mass Transfer 36 (1993) 875–886.
[13] L.S. Oliveira, K. Haghighi, Conjugate heat and mass transfer in convective drying of multiparticle systems. Part I: theoretical considerations. Drying Technol. 16 (1998) 433–461.
[14] L.S. Oliveira, K. Haghighi, Conjugate heat and mass transfer in convective drying of multiparticle systems. Part II: Soybean drying. Drying Technol. 16 (1998) 433–461.
[15] Gh. Juncu, Unsteady forced convection heat/mass transfer around two spheres in tandem at low Reynolds numbers. Int. J. Thermal Sci. 46 (2007) 1011–1022.
[16] R.S. Ramachandran, C. Kleinstreuer, T.-W. Wang, Forced convection heat transfer of interacting spheres. Numer. Heat Transfer A 15 (1989) 471–487.
[17] A. Verma, M.A. Jog, Plasma flow over an array of particles. Int. J. Heat Mass Transfer 43 (2000) 101–111.
[18] A. Maheshwari, R.P. Chhabra, G. Biwas, Effect of blockage on drag and heat transfer from a single sphere and an in-line array of three spheres. Powder Technol. 168 (2006) 74–83.
[19] P.M. Morse, H. Feshbach, Method of Theoretical Physics, II. McGraw-Hill, New York, 1953.
[20] J. Happel, H. Brenner, Low Reynolds Number Hydrodynamics. Nijhoff, Hague, 1984.
[21] E.W. Weisstein, Bispherical Coordinates. MathWorld – A Wolfram Web Resource (2009).http://mathworld.wolfram.com/BisphericalCoordinates.html.
[22] Gh. Juncu, Numerical study of axisymmetric slow viscous flow past two spheres, in: Mathematical Modelling of Environmental and Life Sciences Problems, Proc. 4th Workshop September 2005 Constanta. Academiei, Bucharest, 2006, pp. 109–117.
[23] P.W. Hemker, A Numerical Study of Stiff Two-point Boundary Problems, Ph.D. thesis, Mathematisch Centrum, Amsterdam, 1977.
[24] W. Hackbusch, Multi-Grid Methods and Applications. Springer, Berlin, 1985.